

An integrated microfluidic platform for rapid detection and subtyping of influenza viruses from clinical samples

Chien-Hsuan Tai · Yi-Che Tsai · Chih-Hung Wang ·
Tzong-Shiann Ho · Chih-Peng Chang ·
Gwo-Bin Lee

Received: 7 April 2013 / Accepted: 9 August 2013 / Published online: 1 September 2013
© Springer-Verlag Berlin Heidelberg 2013

Abstract This study reports on the development of an integrated microfluidic system that performs sample pre-treatment, nucleic acid amplification, and optical detection for molecular diagnosis of influenza viruses. The entire analysis protocol including virus lysis, extraction of ribonucleic acid, reverse transcription, polymerase chain reaction, and optical detection was successfully performed using the microfluidic system, which automatically performed the rapid diagnosis and subtyping of the influenza viruses. Signals obtained from an optical detection module could accurately differentiate influenza A/H1 (infA/H1), influenza A/H3 (infA/H3), influenza B (infB), and positive and negative control samples. More importantly, the entire process could be integrated and performed automatically

with less human intervention. The experimental results demonstrated that this developed microfluidic system can successfully distinguish between infA/H1, infA/H3, and infB within 60 min. Furthermore, oral swabs from 92 patients were successfully tested using the developed microfluidic system. Thus, it may be a promising tool for rapid detection of novel and seasonal influenza strains in the near future.

Keywords Microfluidics · Molecular diagnosis · Subtyping · Influenza virus · Magnetic bead · Clinical specimen

Abbreviations

bp	Base pairs
CNC	Computer-numerical-control
cDNA	Complementary DNA
ddH ₂ O	Double-distilled water
dUTP	Deoxyuridine triphosphate
EMVs	Electromagnetic valves
HA	Hemagglutinin
HAU	Hemagglutinin unit
infA/H1	Influenza A/H1
infA/H3	Influenza A/H3
infB	Influenza B
LOD	Limit of detection
MEMS	Micro-electro-mechanical systems
NA	Neuraminidase
NP	Nucleoprotein
PCR	Polymerase chain reaction
PDMS	Polydimethylsiloxane
PMMA	Polymethylmethacrylate
RNA	Ribonucleic acid
RNase	Ribonuclease
RT	Reverse transcription

The preliminary results in this paper were presented at the 2011 International Conference on Miniaturized Systems for Chemistry and Life Sciences (Micro-TAS 2011), Seattle, USA, October 2–October 6, 2011.

C.-H. Tai
Department of Engineering Science,
National Cheng Kung University, Tainan 70101, Taiwan

Y.-C. Tsai · C.-P. Chang (✉)
Department of Microbiology and Immunology,
National Cheng Kung University, Tainan 70101, Taiwan
e-mail: cpchang@mail.ncku.edu.tw

C.-H. Wang · G.-B. Lee (✉)
Department of Power Mechanical Engineering,
National Tsing Hua University, Hsinchu 30013, Taiwan
e-mail: gwobin@pme.nthu.edu.tw

T.-S. Ho
Department of Emergency Medicine,
National Cheng Kung University Hospital, College of Medicine,
National Cheng Kung University, Tainan 70101, Taiwan

RT-PCR	Reverse-transcription polymerase chain reaction
SOIV	Swine-origin influenza virus
TE	Thermoelectric

1 Introduction

The spread of infectious diseases, such as influenza, has become a global health concern. It remains a challenge for any health authority or Center for Disease Control (CDC) to quickly and precisely diagnose diseases in order to control the spread of a novel infectious strain. More seriously, the deaths of 250,000–500,000 people annually worldwide attribute to the spread of influenza, and the number of deaths could increase into the millions in some pandemic years (Simonsen et al. 1997). There are three types of influenza viruses, called A, B, and C, which are commonly categorized based on the antigenic differences between two internal structural proteins known as the nucleoprotein (NP) and the matrix protein (M1) (Webster et al. 1992). Influenza viruses A and B can make human beings severely ill, but influenza C only results in mild symptoms in human beings (Matsuzaki et al. 2006). For instance, various subtypes of influenza A virus infections that have caused severe breakouts have been attributed to influenza pandemics. Influenza A can be further classified by differences in the expressed surface proteins on the viral envelope called hemagglutinin (HA) and neuraminidase (NA). To date, 17 subtypes of HA (H1–H17) and 10 subtypes of NA (N1–N10) have been discovered in different combinations from birds, animals, and human beings (Zhu et al. 2012). However, only three HA subtypes (H1–H3) and two NA subtypes (N1–N2) have been found to infect humans frequently (Alexander et al. 1981). Consequently, the majority of clinical issues associated with seasonal influenza A viruses are associated with these subtypes. For example, the H1N1 subtype that emerged in 1918–1919 was responsible for the Spanish flu pandemic that caused the deaths of 50 million to 100 million people worldwide (Johnson and Mueller 2002). Similarly, the H2N2 pandemic was responsible for the Asian flu in 1957, and the H3N2 pandemic was responsible for the Hong Kong flu that killed one million people worldwide in 1968–1969 (Cox and Subbarao 2000). Furthermore, the first appearance of novel subtypes of the influenza virus has led to high-mortality pandemics. Specifically, the novel H1N1 that appeared in April 2009 has caused serious health concerns (Smith et al. 2009). A new H1N1 virus with a new combination of genes from American pigs, Eurasian pigs, birds, and humans infected people and quickly spread

worldwide, causing a pandemic that was recognized as a swine-origin influenza virus (Medina and Garcia-Sastre 2011). Recently, influenza infections have become one of the most prevalent diseases. Therefore, it is critical to develop a platform for the rapid and accurate diagnosis of influenza infections, especially for subtyping of the influenza viruses, in order to prevent a pandemic outbreak.

Traditionally, the enzyme-linked immunosorbent assay is one of the most commonly used protocols by hospitals and laboratories for clinical diagnosis (Zheng et al. 1990; Siavashi et al. 2005). However, there exist several concerns for this approach. For instance, it involves several labor-intensive processes requiring a series of tedious washing steps. It also has to be performed by well-trained personnel. Currently, immunoassay kits have been commonly used for fast screening of influenza infections (Chambers et al. 1994; Gavin and Thomson 2003). Moreover, their relatively low sensitivity may not meet the needs of practical applications, especially for sensitive detection of clinical or laboratory tests (Hurt et al. 2009; Faix et al. 2009; Vasoo et al. 2009). Therefore, there exists a critical need to develop systems that can simplify, expedite, and miniaturize the detection of influenza infections.

Alternatively, molecular detection may provide a more sensitive and selective diagnosis. Traditional reverse-transcription polymerase chain reaction (RT-PCR) and slab-gel electrophoresis can be used for detection of an influenza infection (Atmar et al. 1996; Smith et al. 2003; Hindiyeh et al. 2005). However, it usually takes more than 4 h for gene amplification, separation of the amplified DNA segments, and detection. Furthermore, tedious sample pretreatment steps such as virus isolation and RNA extraction are still labor-intensive and time-consuming processes. Therefore, there is a great need to develop a new platform to automate and to quickly perform these above-mentioned processes.

For a conventional molecular diagnosis assay, a critical issue was that the RNA samples were easily degraded by the surrounding RNases (Chirgwin et al. 1979; Chomczynski 1993). Therefore, there is a great need to develop a rapid and efficient extraction method to collect RNA from the viruses. Furthermore, the entire process should be integrated and performed automatically with less human intervention. Recently, various methods for extracting RNA have been reported (Akin et al. 1998; Cao et al. 2003; Li et al. 2006). For instance, in order to reduce the labor-intensive process necessary to obtain high-quality RNA, magnetic beads have been widely employed for RNA extraction (Choi et al. 2000; Huang et al. 2002; Gijs 2004; Li et al. 2008). Recently, specific nucleotide probes conjugated onto the surface of magnetic beads by utilizing the carboxylated linkage (Hawkins et al. 1994) have been integrated into microfluidic systems to enhance their

performance. Due to the fact that high surface-to-volume ratio of the magnetic beads selectively modified with a variety of detection targets, the application of oligonucleotide-conjugated magnetic beads for isolation of specific nucleic acid sequences involved DNA hybridization (Jungell-Nortamo et al. 1988) can be greatly improved. Hence, sequence-specific hybridization capture on magnetic beads can be further easily manipulated, sorted, and concentrated in the microfluidic systems. Therefore, more bead-based assays have been extensively employed recently on microfluidic systems (Lien et al. 2009; Liu et al. 2009; McCalla et al. 2012). In comparison with the conventional method (Chomczynski and Mackey 1995), the extraction of RNA samples can be stably extracted and easily performed by applying an external magnetic field.

In the recent years, micro-electro-mechanical systems (MEMS) technology has been extensively employed for lab-on-a-chip (LOC) applications. These microfluidic systems comprised interconnected fluidic microchannel networks, microvalves, micromixers, micropumps, and reaction chambers may perform many of the required protocol steps (Auroux et al. 2002; Grodzinski et al. 2004; Vilknér et al. 2004). In the past two decades, LOCs that can provide even superior performance when compared with their large-scale counterparts have been successfully demonstrated. For instance, our previous study showed that sample pretreatment of viruses could be performed using a microfluidic system (Wang et al. 2012). However, it was relatively costly since it used fluorescent TaqMan probes. Furthermore, optical detection was still challenging to integrate into a single system, which is crucial for fast and accurate diagnosis of viruses.

In this study, we therefore develop a microfluidic system for automatic detection of influenza viruses in patient samples. The microfluidic system consists of a microfluidic control module for the transport of small amount of fluids, a magnet for magnetic isolation of RNA, a temperature control module equipped with a thermoelectric (TE) cooler, and an optical detection module with a fluorescent dye (SYBR Green dye) for detecting the amplified RT-PCR products. Current MEMS and microfluidic systems that detect influenza usually suffer from limited sample processing capability, as they typically detect only the presence of a single target at a time. Since the diagnosis, as well as the administration of treatments for influenza infections, requires the testing of multiple potential viruses (e.g., infA/H1, infA/H3, and infB), these existing systems are thus insufficient as realistic diagnostics. To overcome this limitation, the developed microfluidic system may perform parallel assays to simultaneously detect and subtype infA/H1, infA/H3, and infB while also including the three positive controls and one negative control as assay verification. Note that we used three types of DNA for the positive

controls, one infA/H1-positive test, one infA/H3-positive test, and one infB-positive test. More importantly, this microfluidic system is capable of performing the entire assay, including virus lysis, RNA extraction, reverse transcription, polymerase chain reaction, and integrated optical detection in a completely automated fashion. As a further improvement, this new magnetic-bead-based microfluidic system could rapidly diagnose and subtype various influenza viruses within 60 min, which has shortened the assay time by approximately 45 % when compared to our previous study (110 min). Using patient samples, this microfluidic system showed a higher accuracy and was more time-efficient. Totally, 92 clinical specimens were successfully tested. An oral swab from a patient with suspected influenza infections can be rapidly detected using the microfluidic system. Using this approach, the results from this study revealed that the analysis can be automatically performed with a smaller biosample (10 μ L), and less sample/reagent consumption in a shorter period of time (within 60 min).

2 Materials and methods

2.1 Experimental process

Magnetic beads (stock concentration = 4×10^8 beads/mL, bead diameter = 4.5 μ m, Dynabeads[®] Myone[™] Carboxylic Acid, Invitrogen, USA) conjugated with various subtype-specific nucleotide probes including an infA/H1 probe (5'-TTTTTTTTTTAGACACAATATGTATAGGCTACCATG-3'), an infA/H3 probe (5'-TTTTTTTTTTA GAATAAGCATCTATTGGACAATAGT-3'), and an infB probe (5'-TTTTTTTTTTACTACTCATGGTAGTAACATCCAATG-3') were first loaded into the sample chambers, respectively (Fig. 1a; Wang et al. 2012). A temperature of 95 °C was then applied to lyse the viruses using a temperature control module, followed by hybridizing the released viral RNA with the oligonucleotide probes, which were conjugated onto the surface of the magnetic beads at a temperature of 60 °C (Fig. 1b). Then, the magnetic beads with the attached viral RNA were magnetically purified (Fig. 1c). The RNA was then reverse-transcribed into DNA (Fig. 1d), followed by a nucleic acid amplification step (Fig. 1e) using the same temperature control module. Finally, the amplified RT-PCR products were detected by an optical detection module (Fig. 1f) using a SYBR Green dye.

2.2 Chip design and fabrication process

Figure 2a shows an exploded view of the integrated microfluidic chip consisting of two polydimethylsiloxane (PDMS, Sylgard 184A/B, Dow Corning Corp., USA) layers and one glass plate. The developed microfluidic chip was

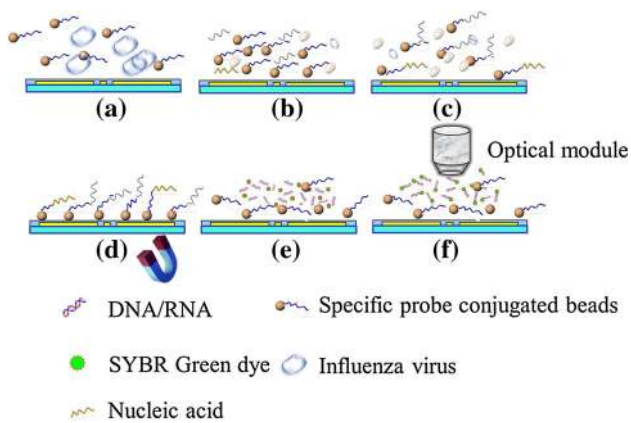


Fig. 1 A schematic illustration of the operating process performed on the integrated microfluidic chip

designed for performing sample pretreatment, nucleic acid amplification, and optical detection for molecular diagnosis of influenza viruses. The entire process including virus lysis, extraction of RNA, a one-step RT-PCR process, and optical detection was integrated into the microfluidic chip, which automatically performed the rapid diagnosis and subtyping of the influenza virus. Table 1 lists the detailed protocol and the operating conditions for each process step. The developed microfluidic chip consisted of a two-layer PDMS structures (i.e., a thick PDMS layer and thin PDMS layer) and one glass substrate, as schematically shown in Fig. 2b. Two major components integrated in this chip were normally closed microvalves (Yang et al. 2009) and four suction-type micropumps (Weng et al. 2011a, b). Note that the four suction-type micropumps were used for one *inflA*/H1 test, one *inflA*/H3 test, one *inflB* test, and one negative control test. Both of them were fabricated using microfabrication processes. Briefly, the master molds with microfluidic structures on polymethylmethacrylate were formed using a computer-numerical-control machining process (EGX-400, Roland Inc., Japan) equipped with a 0.5-mm drill bit (Yang et al. 2009). Utilizing a PDMS replication technique, the inverse microstructures of the fluidic channels and the air chambers could be obtained. The thick-film PDMS layer and thin-film PDMS layer were then bonded together using an oxygen plasma treatment. Finally, a soda-lime glass substrate (G-Tech Optoelectronics Corp., Taiwan) was bonded with the PDMS structures to form the microfluidic chip. A photograph of the integrated microfluidic chip, which can automatically perform the entire analysis process, is shown in Fig. 2c. The dimensions of the chip were measured to be 7.5 cm × 5.9 cm.

2.3 Working principle

The working principle of the suction-type micropump is schematically illustrated in Fig. 3. The driving force for

liquid transport is the negative gauge pressure that creates a suction force. Figure 3a shows the initial state of the suction-type micropump. The sample fluid was first loaded into the inlet chamber. Figure 3b shows the deflections of the PDMS membranes when there was a negative gauge pressure in the air chambers, such that the fluidic sample could be drawn into the fluidic reservoir. Then, the normally closed microvalve on the left side was released when the normally closed microvalve on the right side was switched on (Fig. 3c). With this approach, the floating-block structure in the left microchannel can be switched off to push the sample forward. Next, all the PDMS membranes of the micropump and the right normally closed microvalve were released to push the liquid forward into the outlet chamber (Fig. 3d). The activation time of each step was set to be 1 s. Therefore, a total of 3 s per cycle was used. Digital signals from a custom-made control circuit were used to regulate electromagnetic valves (EMVs, SMC Inc., S070M-5BG-32, Japan) to control the motion of these membranes. Detailed information about this micropump could be found in our previous work (Weng et al. 2011a, b). In this study, the integrated microfluidic system that can perform the entire process for the detection of influenza viruses has been demonstrated. It can carry out multiple reactions for multiple detections of influenza viruses. Successful demonstration for the rapid detection and subtyping of influenza viruses from clinical samples has been achieved using the developed microfluidic system.

2.4 Custom-made system

Figure 4a shows a schematic illustration of the microfluidic detection system. The custom-made system consists of an air compressor (UN-90 V, UNI-CROWN Inc., Taiwan) equipped with several EMVs (S070M-5BG-32, SMC Inc., Japan) to control the motion of the PDMS membranes for transport fluids, a magnet to collect the magnetic beads for purification of RNA, and a temperature control module (USB4718, Advantech Corp., Taiwan) equipped with a thermoelectric (TE) cooler (TEC1-127.10, TANDE Corp., Taiwan) for RT-PCR thermal process, and an optical detection module is comprised of a laser (MBL5, CNI Corp., China) to excite fluorescent dyes, a band-pass filter (525/20 BP, Chroma Technology Corp., USA) and a dichroic mirror (505LP, Chroma Technology Corp., USA) to filter light with wavelengths ranging from 515 to 535 nm, a PMT (R928, Hamamatsu Corp., Japan) for the collection of fluorescent signals, a collimating lens (NT45-233, ONSET ELECTRO-OPTICS Corp., Taiwan) to focus the lights, and a data acquisition card (USB4716, Advantech Corp., Taiwan) to transform fluorescent signals into electronic signals. The dimensions of the custom-made

Fig. 2 a An exploded view of the integrated microfluidic chip. It consisted of two PDMS layers and one glass plate. **b** A schematic illustration of the integrated microfluidic chip consisting of a thick-film PDMS layer, a thin-film PDMS layer, and a glass substrate. **c** A photograph of an assembled microfluidic chip. The dimensions of the chip were measured to be 7.5 cm × 5.9 cm (length × width)

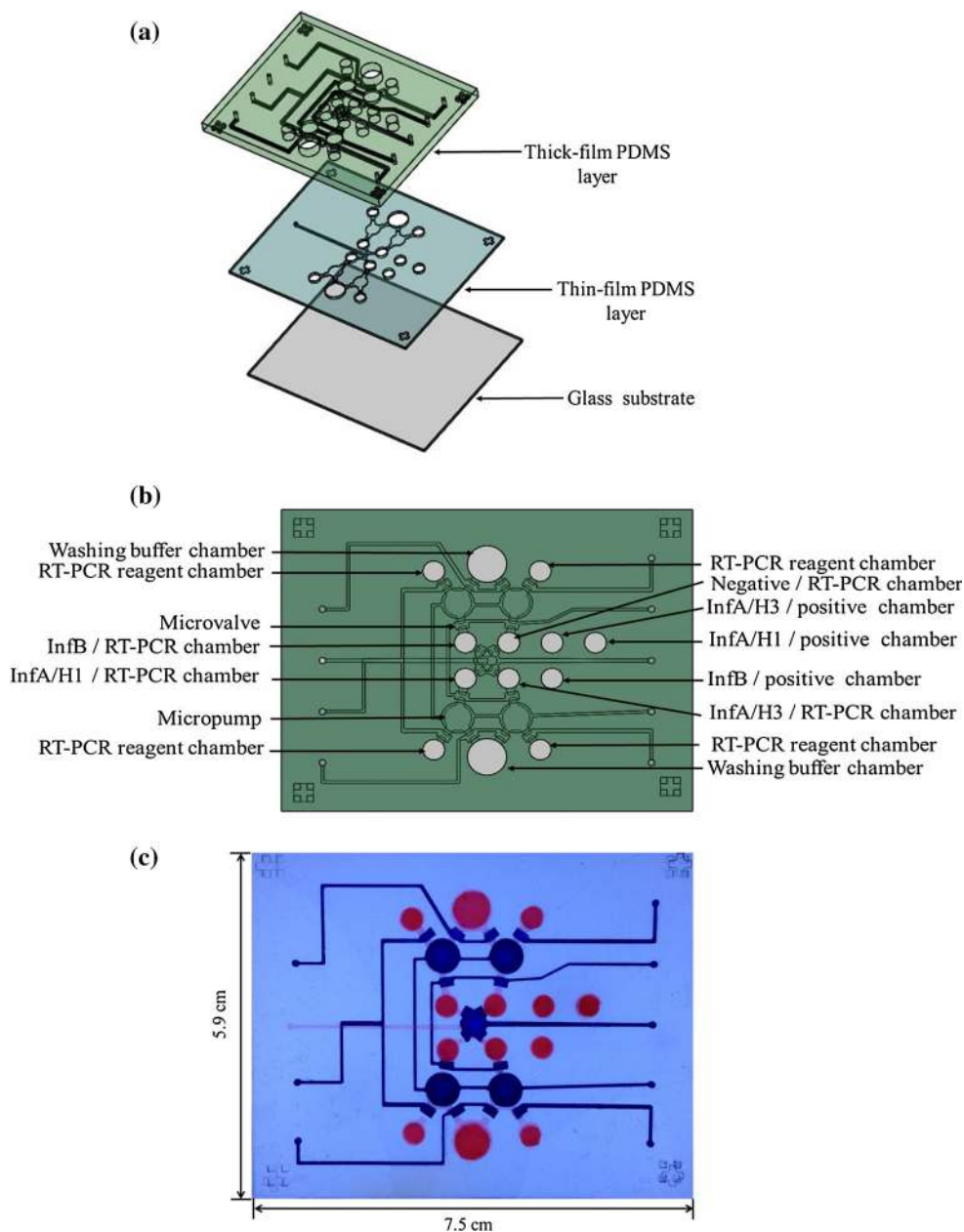


Table 1 A detailed comparison of the detailed experimental protocol performed on the microfluidic chip

Operation	Samples/reagents	Volume (μL)	Temperature	Time
Virus lysis	Virus/clinical specimens	10	95 °C	5 min
Hybridization	Magnetic beads	10	60 °C	10 min
Sample isolation	Washing buffer (ddH ₂ O)	200	Room temperature	2 min
One-step RT-PCR	RT-PCR reagents	20	42 °C (RT step)	5 min
			95 °C (initial denaturing step)	5 min
			95 °C (denaturation)	3 s
			58 °C (annealing)	20 s
			72 °C (extension)	1 s
Optical detection			Room temperature	3 min

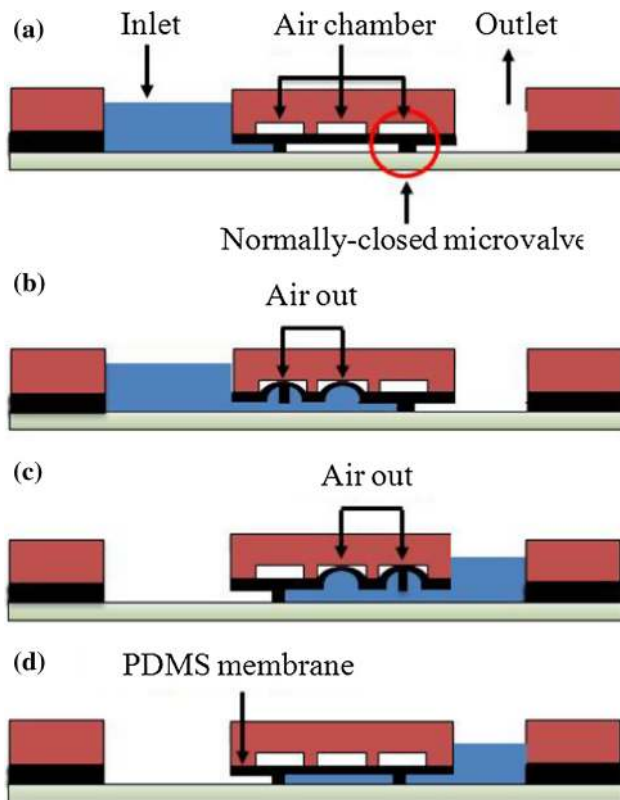


Fig. 3 The working principle for the micropump. **a** The initial state of the suction-type micropump. **b** The PDMS membranes were deflected by the negative gauge pressure in the air chambers. **c** The normally closed microvalve on the *left-hand side* was released when the normally closed microvalve on the *right-hand side* was switched on. **d** With this approach, the floating-block structure in the left microchannel can be switched off to push the sample forward. Next, all of the PDMS membranes of the micropump and right normally closed microvalve were released to push the liquid forward into the outlet chamber

system were measured to be $45 \times 40 \times 35$ cm, as shown in Fig. 4b. The magnet could be controlled to place underneath the microfluidic chip during the operation.

2.5 Virus preparation

InfA/H1 (a subtype of H₁N₁, 95N2H1), InfA/H3 (a subtype of H₃N₂, A/California/7/2004), and InfB (94N399IB) were first mixed in serum separately and then added to washed, near-confluent (90 %) monolayers of Madin-Darby canine kidney (MDCK) cells and incubated at 35 °C with 5 % CO₂. The virus/serum mixture was then replaced with a serum-free medium supplemented with 0.05 % Trypsin-EDTA (Invitrogen™, USA), and the cells were incubated at 35 °C with 5 % CO₂. After harvesting the supernatant from the culture medium, this virus-containing culture supernatant was stored at –80 °C prior to usage. The initial titers of the stock of the three viruses were measured to be 1.28 hemagglutinin units (HAU). All operations were

carried out according to the safety instructions provided by the National Institutes of Health in Taiwan.

Clinical specimens were obtained from the Microbiology and Immunology Laboratory of National Cheng Kung University (NCKU) in Taiwan and the Department of Pathology of NCKU Hospital in Taiwan. These clinical specimens were stored at –80 °C until tested. A total of 92 clinical samples were collected, 30 of which were known negative samples and the other 62 samples were known positive samples.

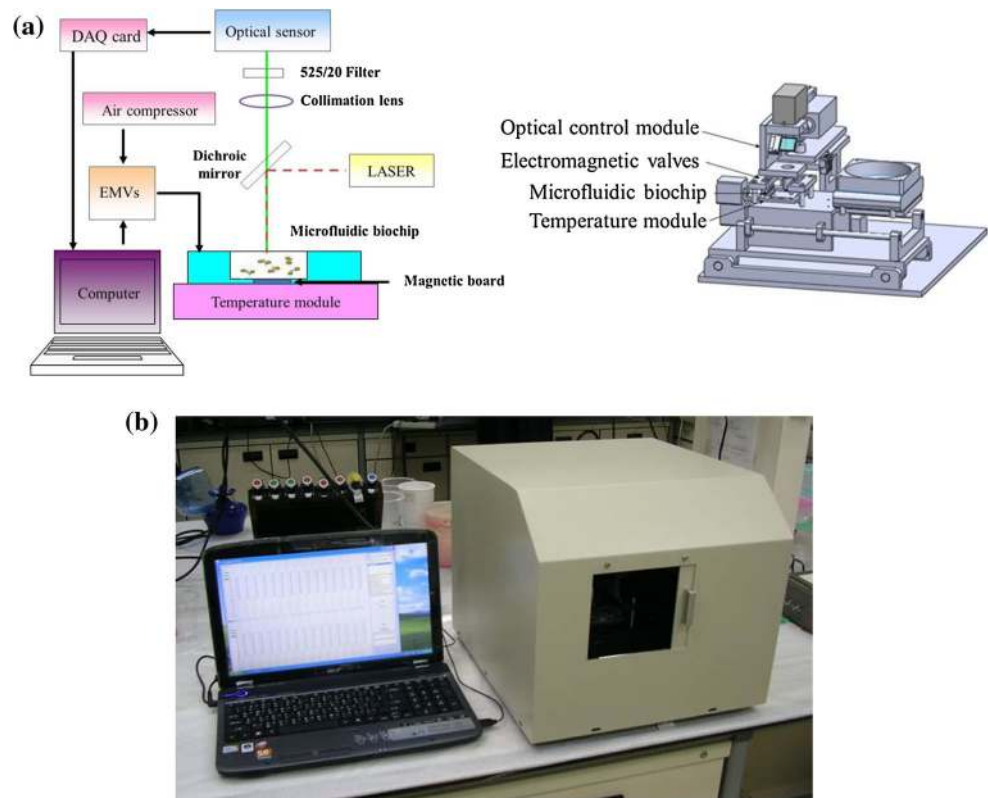
2.6 Positive control

The cloning protocol followed the user guide for the TOPO TA cloning® kit (Invitrogen Co., USA). The RT-PCR products were used by using specific forward/reverse primer pairs to amplify the HA gene of infA/H1, infA/H3, and infB. All 6 μL cloning mixtures contained 4 μL of freshly made PCR products, 1 μL of TOPO® vector, and 1 μL of salt solution. The mixture was gently mixed and incubated for 5 min at room temperature. One tube of Shot® *E. coli* cell was thawed on ice. Two microliters of cloning mixture was added to Shot® *E. coli*, mixed gently, and put on ice. All of the mixtures were incubated on ice for 30 min and heat-shocked for 30 s at 42 °C without shaking. Finally, 250 μL of LB broth was added to the transformation mixture and shaking continuously at 37 °C for 1 h. Fifty microliters of this transformation solution was then spread on a LB-Amp (ampicillin 100 mg/mL, Sigma Co., USA) plate and then incubated overnight at 37 °C. The transformants were finally selected and analyzed by a subtype-specific PCR for the detection of influenza virus.

2.7 One-step RT-PCR protocol

PCR amplification is a well-known method for the amplification of nucleic acids and can be used to verify whether the released RNA can be stably extracted and converted to stable complementary DNA (cDNA). In this study, a one-step RT-PCR with hydrolysis probes was applied to the diagnosis of various RNA viruses. The RNA purified either from patient samples or from cultured laboratory samples was further examined using a commercial kit (KK4660 KAPA SYBR® FAST One-Step qRT-PCR kit, ABI Prism™, USA). All the RT-PCR processes were performed using the temperature control module equipped with a TE cooler, which was placed underneath the microfluidic chip. Twenty microliters of reaction reagents was used, which was composed of 5 μL of bead-captured viral RNA sample, 10 μL of KAPA SYBR FAST qPCR Master Mix (2×), 0.4 μL of deoxyuridine triphosphate (dUTP, 10 mM), 0.4 μL of KAPA RT Mix (50×), 0.4 μL of each primer for InfA/H1, InfA/H3, and InfB forward/

Fig. 4 **a** A schematic illustration of the microfluidic detection system. **b** The dimensions of the custom-made system were measured to be $45 \times 40 \times 35$ cm



reverse primers (Wang et al. 2012), and 3.4 μL of double-distilled water (ddH_2O). The reaction reagents were first loaded into the RT-PCR chamber and were pumped to the reaction chamber. The cDNA synthesis process at 42 $^\circ\text{C}$ for 5 min was followed by thermocycling processes, which included an initial denaturing step at 95 $^\circ\text{C}$ for 5 min, then denaturing at 95 $^\circ\text{C}$ for 3 s, annealing at 58 $^\circ\text{C}$ for 20 s, and extension at 72 $^\circ\text{C}$ for 1 s for a total of 40 cycles. Finally, the amplified RT-PCR products were detected by an integrated optical detection module.

For the negative control, the template RNA was replaced by RNase-free water. In order to confirm the PCR process, we used three types of DNA for the positive controls, which were cloned from hemagglutinin fragment of InfA/H1 (2.68 $\mu\text{g}/\text{mL}$), InfA/H3 (2.43 $\mu\text{g}/\text{mL}$), and InfB (2.05 $\mu\text{g}/\text{mL}$), respectively. Twenty microliters of the reaction reagents was used, which was composed of 1 μL of the positive-control DNA sample, 10 μL of KAPA SYBR FAST qPCR Master Mix (2 \times), 0.4 μL of dUTP (10 mM), 0.4 μL of KAPA RT Mix (50 \times), 0.4 μL of each primer for InfA/H1, InfA/H3, and InfB forward/reverse primers, and 7.4 μL of ddH_2O . These control samples were loaded into the corresponding InfA/H1, InfA/H3, and InfB-positive-control chamber. Note that the signals from the three positive controls (InfA/H1, InfA/H3, and InfB) were around 0.834, 0.828, and 0.794 V, respectively. All of the three controls were measured with strong signals using the optical detection module for confirming our experiments. If

one of their signals is close to one for the negative control (double-distilled water), the platform is not reliable. This indication can improve the reliability of our platform.

The sensitivity and specificity were determined by comparing against a standard, commercially available isolation kit (QIAamp Viral RNA Mini kit, QIAGEN, Germany) obtained from the Microbiology and Immunology Laboratory of NCKU in Taiwan to verify that our developed system achieved comparable results.

3 Results and discussion

3.1 Characterization of the micropump

In this study, an integrated microfluidic chip was designed and fabricated for fast diagnosis and subtyping of influenza viruses. A suction-type micropump incorporated with a normally closed microvalve was adopted for precise liquid delivery such that the entire assay could be automated. The performance of the micropump is crucial for driving the liquid in the integrated microfluidic chip, as described in the previous sections. It is important to explore the relationship between the pumping rate and the applied air pressure when optimizing the operating conditions. Figure 5 shows the relationship between the pumping rate and the applied air pressure of the developed micropump when operated at -20 , -25 , -30 , -40 , -50 , -60 , -70 , and

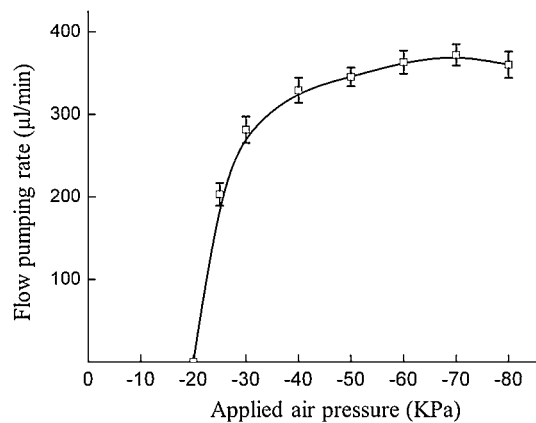


Fig. 5 The relationship between the pumping rate and the air pressure applied to the micropump

–80 kPa, respectively. The pumping rate could be as high as $372.24 \pm 15.95 \mu\text{L}/\text{min}$, when actuated at a pressure of –70 kPa. Considering a reproducible pumping rate, the suction-type micropump was activated at a pressure of –50 kPa, corresponding to a pumping rate of $345.46 \pm 11.14 \mu\text{L}/\text{min}$ in the subsequent experiments. Note that the error bars shown in Fig. 5 were obtained from three repeated measurements.

3.2 Selectivity test

In order to test the selectivity of the probe-conjugated magnetic beads, the specific nucleotide probes for infA/H1 (1.28 HAU), infA/H3 (1.28 HAU), and infB (1.28 HAU) were used for the extraction of viral RNA and hybridization with infA/H1 (lane 1), infA/H3 (lane 5), and infB (lane 9) strains, respectively, as shown in Fig. 6a. These experimental results demonstrated excellent selectivity to infA/H1, infA/H3, and infB with extremely high optical signals, 0.612 ± 0.027 , 0.785 ± 0.013 , and $1.112 \pm 0.018 \text{ V}$, respectively. In addition, Fig. 6a also shows that the infA/H1 probe-conjugated beads incubated with infA/H3 and infB isolates (lanes 2 and lane 3) or infA/H3 probe-conjugated beads incubated with the infA/H1 and infB isolates (lane 4 and lane 6) or infB probe-conjugated beads incubated with the infA/H1 and infA/H3 isolates (lane 7 and lane 8) could not generate PCR products, as indicated by detection signals close to the negative control level (lane 2, lane 3, lane 4, lane 6, lane 7, lane 8, and NC were 0.194 ± 0.011 , 0.201 ± 0.026 , 0.199 ± 0.024 , 0.186 ± 0.015 , 0.194 ± 0.014 , 0.212 ± 0.022 , and $0.180 \text{ V} \pm 0.012$, respectively). Note that the error bars shown here were obtained from three repeated measurements.

In order to confirm the validity of the optical signals from the developed integrated chip, the RT-PCR products were also visualized by using gel electrophoresis on a 2 % agarose gel with ethidium bromide staining. Figure 6b

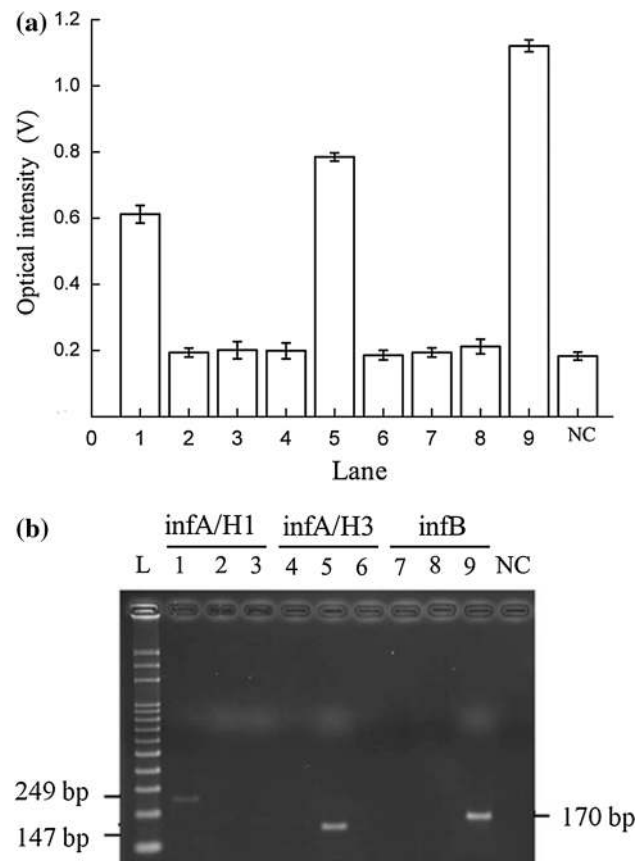


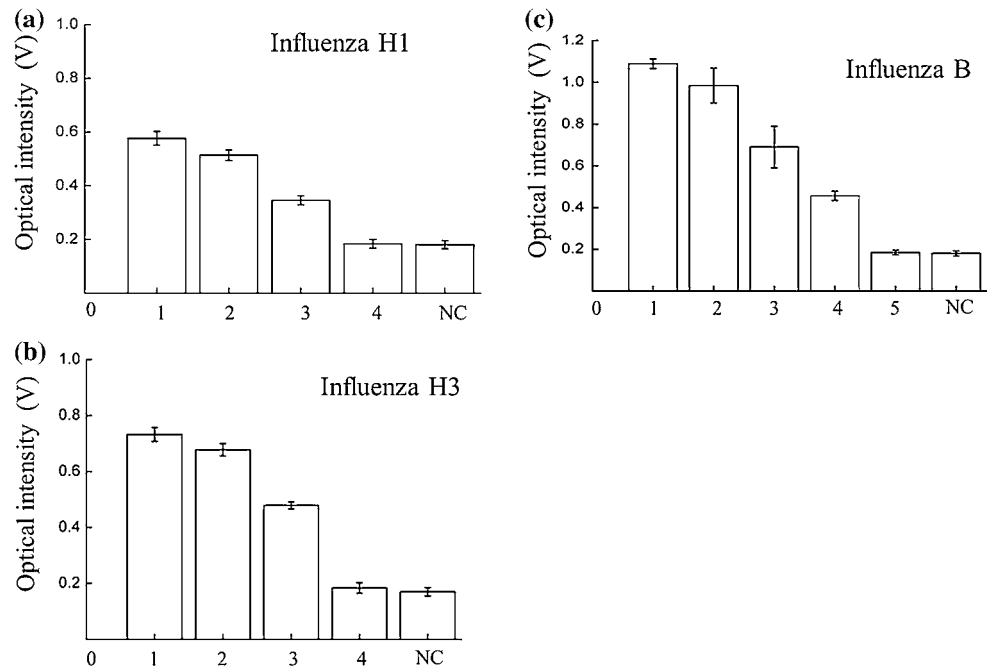
Fig. 6 a Selectivity results for the microfluidic chip by using the optical detection module. **b** The length of the infA/H1, infA/H3, and infB detection genes were 249, 147, and 170 bp, respectively. The results showed that infA/H1, infA/H3, and infB probes were highly specific to subtyping of influenza viruses

shows a gel image of the PCR products amplified from the DNA transcribed from the total RNA that was extracted using the super-paramagnetic-bead-based method (Wang et al. 2012). The length of the detection genes for infA/H1, infA/H3, and infB were 249, 147, and 170 base pairs (bp), respectively. Note that lane L used a 100-bp DNA ladder marker and lane NC used ddH₂O as a template. These results showed that the infA/H1, infA/H3, or infB probes provided a high selectivity for subtyping of influenza viruses and only the expected subtypes of samples were amplified successfully. No cross-reactivity was observed among infA/H1, infA/H3, and infB viruses, thus demonstrating high specificity by using the subtype-specific primers/probe.

3.3 Limit of detection of the integrated microfluidic system

In order to explore LOD of the developed microfluidic chip, three experiments were performed. Purified virus cultured in the laboratory was first used to test for the LOD.

Fig. 7 Sensitivity results for the microfluidic chip by using the optical detection module; different concentrations of influenza A/H1, influenza A/H3, and influenza B viruses diluted from a sample with an initial concentration of 12.8 HAU/5 μ L were tested. **a** A series of images of the magnetic complexes with different viral concentrations of influenza A/H1 when operated by the microfluidic chip, **b** optical signals from the detection of influenza A/H3 at different concentrations in the microfluidic chip, **c** optical signals from the detection of influenza B at different concentrations



Four different concentrations of infA/H1 viruses, specifically lane 1 (1.28 HAU), lane 2 (0.128_HAU), lane 3 (0.0128 HAU), and lane 4 (0.00128 HAU), were loaded into the integrated microfluidic chip, as shown in Fig. 7a. The optical signals for the various infA/H1 concentrations were measured to be 0.576 ± 0.026 , 0.513 ± 0.019 , 0.346 ± 0.017 , and 0.183 ± 0.016 V, respectively. Note that the signal for the negative control was around 0.180 ± 0.015 V. Note that the error bars shown here were obtained from three repeated measurements. Experimental results demonstrated that the detection limit of this microsystem was found to be a 10^2 dilution of 1.28 HAU of infA/H1 (0.0128 HAU). In order to confirm the validity of the optical signals from the developed integrated chip, Fig. 8a shows a gel image of the amplified PCR products for comparison. Note that the length of the infA/H1 detection gene was 249 bp and the lane L used a 50-bp DNA ladder marker. Lanes 1, 2, 3, and 4 were 1.28, 0.128, 0.0128, and 0.00128 HAU, respectively, and lane NC used ddH₂O as a template.

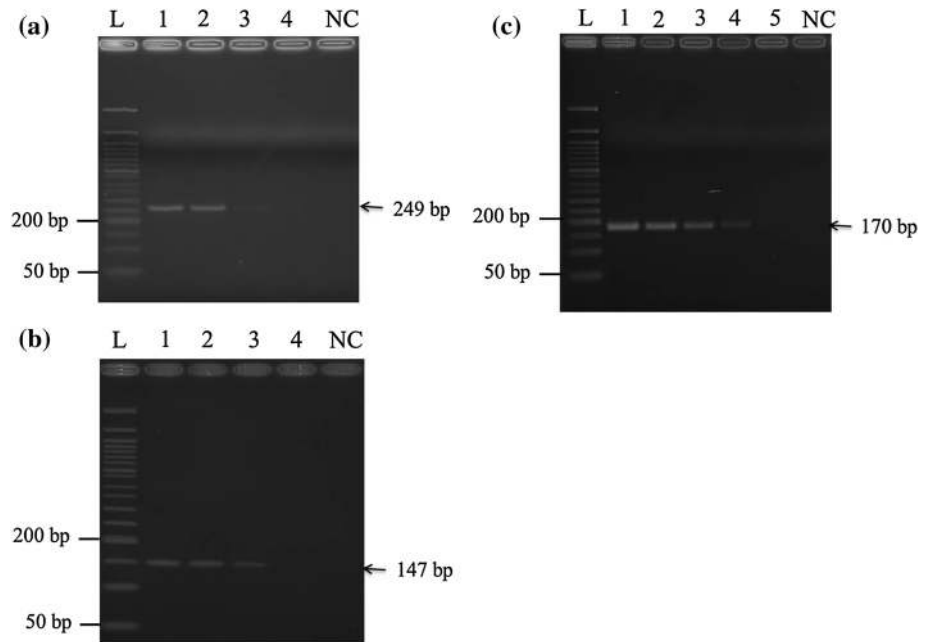
Similarly, four different concentrations of infA/H3 viruses, specifically lane 1 (1.28 HAU), lane 2 (0.128_HAU), lane 3 (0.0128 HAU), and lane 4 (0.00128 HAU), were loaded into the integrated microfluidic chip to test the LOD for InfA/H3, as shown in Fig. 7b. The optical signals from the infA/H3 samples were measured to be 0.732 ± 0.025 , 0.678 ± 0.022 , 0.479 ± 0.012 , and 0.180 ± 0.018 V, respectively. Note that the signal from the negative control was around 0.174 ± 0.011 V. The error bars shown were obtained from three repeated measurements. These experimental results revealed that the

LOD of the microsystem was a 10^2 dilution of 1.28 HAU (0.0128 HAU) for infA/H3. Similarly, in order to confirm the validity of the optical signals from the integrated chip, Fig. 8b shows a gel electrophoresis image of the amplified PCR products amplified for comparison. Note that the length of the infA/H3 detection gene was 147 bp and the lane L used a 50-bp DNA ladder marker. Lanes 1, 2, 3, and 4 were 1.28, 0.128, 0.0128, and 0.00128 HAU, respectively, and lane NC used ddH₂O as a template.

In addition, five different concentrations of infB viruses, specifically lane 1 (1.28 HAU), lane 2 (0.128 HAU), lane 3 (0.0128 HAU), lane 4 (0.00128 HAU), and lane 5 (0.000128 HAU), were loaded into the integrated microfluidic chip to test the LOD, as shown in Fig. 7c. The optical signals for infB were measured to be 1.089 ± 0.023 , 0.985 ± 0.083 , 0.690 ± 0.015 , 0.457 ± 0.092 , and 0.185 ± 0.031 V, respectively. Note that the signal for the negative control was around 0.181 ± 0.042 V. The error bars shown were obtained from three repeated measurements. These experimental results demonstrated that the detection limit of the microsystem was a 10^3 dilution of 1.28 HAU for infB (0.00128 HAU). Again, in order to confirm the validity of the optical signals from the developed integrated chip, Fig. 8c shows a gel electrophoresis image of the amplified PCR products. Note that the length of the infB detection gene was 147 bp and the lane L used a 50-bp DNA ladder marker. Lanes 1, 2, 3, 4, and 5 were 1.28, 0.128, 0.0128, 0.00128, and 0.000128 HAU, respectively, and lane NC used ddH₂O as a template.

To convert the HAU values of virus samples to copy numbers, viral RNA was extracted from the virus samples,

Fig. 8 Sensitivity results for the microfluidic chip by using slab-gel electrophoresis. **a** Gel image of the amplified PCR products; note that the length of the infA/H1 detection gene was 249 bp. **b** Gel image of the amplified PCR products. Note that the length of the infA/H3 detection gene was 147 bp. **c** Gel image of the amplified PCR products. Note that the length of infA/H1 was 170 bp



measured by a spectrophotometer, and calculated based on the established relationship (Witthaya et al. 2011). The extraction of total RNA from the virus samples was performed by using the QIAamp Viral RNA Mini kit (QIAGEN, Germany). The concentrations of the extracted total RNA were determined by a spectrophotometer (Beckman, DU530 UV/Vis, USA). The copy numbers of RNA were then calculated by the following formula (Kamol et al. 2008).

The number of RNA copy (copy)

$$= \frac{[\text{RNA concentration (g)} \times 6.02 \times 10^{23}]}{[\text{length of in vitro RNA (bp)} \times 340]}.$$

Initial concentrations of the three viruses (infA/H1, infA/H3, and infB) at 128 HAU were then calculated to be 1.6×10^8 , 1.0×10^8 , and 2.7×10^8 copies, respectively. Therefore, our HAU results can be converted to copy numbers. Experimental results for the LOD of infA/H1, infA/H3, and infB were measured to be 1.6×10^3 , 1.0×10^3 , and 2.7×10^2 copies, respectively. Our results showed acceptable LOD in comparison with many reports or kits (Boonsuk et al. 2008). Note that the previous studies (Payungporn et al. 2006; Li et al. 2006; Thontiravong et al. 2007; Zhang and Xing 2010) showed that the LODs of influenza diagnosis were between 10 and 10^4 copies by using purified viral RNA samples.

3.4 Diagnosis of influenza infections using clinical specimens

According to the aforementioned experimental conditions and the promising characterization results from the

Table 2 Two-by-two table for the influenza A/H1 test

Operating process	Microfluidic chip	
	Positive	Negative
Tested positive	9	0
Tested negative	1	10

$$\text{Sensitivity} = 9/(9 + 1) = 0.9; \text{ specificity} = 10/(0 + 10) = 1.0$$

Table 3 Two-by-two table for the influenza A/H3 test

Operating process	Microfluidic chip	
	Positive	Negative
Tested positive	33	0
Tested negative	3	10

$$\text{Sensitivity} = 33/(33 + 3) = 0.9; \text{ specificity} = 10/(0 + 10) = 1.0$$

Table 4 Two-by-two table for the influenza B test

Operating process	Microfluidic chip	
	Positive	Negative
Tested positive	20	0
Tested negative	2	10

$$\text{Sensitivity} = 20/(20 + 2) = 0.9; \text{ specificity} = 10/(0 + 10) = 1.0; \text{ note that total number of positive samples (H1 (9), H3 (33), INB (20)) was 62}$$

integrated microfluidic chip, clinical specimens were next tested. The microfluidic chip was designed with multiple detection regions, three positive tests, and one negative test. Ninety-two specimens were tested using the

prototype microfluidic chips. The sensitivity and specificity were determined by comparing against gold standards (QIAamp Viral RNA Mini kit, QIAGEN, Germany) obtained from the Microbiology and Immunology Laboratory of NCKU in Taiwan and the Department of Pathology of NCKU Hospital in Taiwan to verify that our developed system achieved comparable results. Table 2 shows the summary of the infA/H1 test results. A sensitivity of 90 % and a specificity of 100 % were verified. Similarly, Table 3 shows the summary of the infA/H3 test results. A sensitivity of 91 % and a specificity of 100 % were verified. Table 4 shows the summary of the infB test results. A sensitivity of 90 % and a specificity of 100 % were verified accordingly. The entire experimental protocol was performed automatically within 60 min, and all the results showed that the developed microfluidic chip could detect clinical samples successfully with a high specificity and sensitivity. It therefore has several advantages when compared with the gold standard, including reduced consumption of biosamples (10 μ L) and reagents (215 μ L), automation, and a shorter time (within 60 min) for analysis. Note that the gold standard required 140 μ L of biosamples and 2,810 μ L of reagents and took about 100 min.

4 Conclusion

In this study, an integrated microfluidic system with the capability to automatically perform viral lysis, RNA extraction, a one-step RT-PCR process, and optical detection was successfully demonstrated. The RNA was successfully purified from viruses and clinical specimens utilizing the proposed magnetic-bead-based method within the microfluidic system. Compared to a conventional method (QIAamp Viral RNA Mini kit, QIAGEN, Germany) that required 100 min to perform the entire RNA isolation, nucleic acid amplification, and detection steps, our prototype microfluidic system could perform the entire process within 60 min. Moreover, the system performed the entire process automatically, making it less labor-intensive and greatly reducing the risk of contamination of the results or risk of infection to the operator. Furthermore, the subtyping of the influenza viruses could be realized on this developed system. In conclusion, our developed microfluidic system may provide a powerful alternative platform for fast diagnosis of influenza viruses.

Acknowledgments The authors would like to thank the National Science Council in Taiwan for financial support (NSC101-2120-M-007-014). Partial financial support from the Towards a World-Class University Project is also greatly appreciated.

References

- Akin A, Wu CC, Lin TL (1998) A comparison of two RNA isolation methods for double-stranded RNA of infectious bursal disease virus. *J Virol Methods* 74:179–184
- Alexander DJ, Assaad F, Bachmann PA, Bögel K, Chu H, Easterday BC, Hannoun CM, Kaplan MM, Laver WG, Ottis K, Romvary JJ, Scholtissek C, Shortridge KF, Slepukin AN, Tumova B, Webster RG (1981) The ecology of influenza viruses: a WHO memorandum. *Bull World Health Organ* 59(6):869–873
- Atmar RL, Baxter BD, Dominguez EA, Taber LH (1996) Comparison of reverse transcription-PCR with tissue culture and other rapid diagnostic assays for detection of type A influenza virus. *J Clin Microbiol* 34(10):2604–2606
- Auroux PA, Iossifidi D, Reyes DR, Manz A (2002) Micro total analysis systems. 2. Analytical standard operations and applications. *Anal Bioanal Chem* 74:2637–2652
- Boonsuk P, Payungporn S, Chieochansin T, Samransamruajkit R, Amonsin A, Songserm T, Chaisingh A, Chamnanpood P, Chutinimitkul S, Theamboonlers A, Poovorawan Y (2008) Detection of influenza virus types A and B and type A subtypes (H1, H3, and H5) by multiplex polymerase chain reaction. *Tohoku J Exp Med* 215(3):247–255
- Cao QF, Meng YP, Sun Y (2003) An effective quick method for total RNA extraction in *Malus*. *J Agric Biotechnol* 11(4):428–429
- Chambers TM, Shortridge KF, Li PH, Powell DG, Watkins KL (1994) Rapid diagnosis of equine influenza by the Directigen FLU-A enzyme immunoassay. *Vet Rec* 135(12):275–279
- Chirgwin JM, Przybyla AE, MacDonald RJ, Rutter WJ (1979) Isolation of biologically active ribonucleic acid from sources enriched in ribonuclease. *Biochemistry* 18:5294–5299
- Choi JW, Ahn CH, Bhansali S, Henderson HT (2000) A new magnetic bead-based, filterless bio-separator with planar electromagnet surfaces for integrated bio-detection systems. *Sens Actuators B Chem* 68:34–39
- Chomczynski P (1993) A reagent for the single-step simultaneous isolation of RNA, DNA and proteins from cell and tissue samples. *Biotechniques* 15:532–537
- Chomczynski P, Mackey K (1995) Short technical report. Modification of the TRIZOL reagent procedure for isolation of RNA from Polysaccharide-and proteoglycan-rich sources. *Biotechniques* 19(6):942–945
- Cox NJ, Subbarao K (2000) Global epidemiology of influenza: past and present. *Annu Rev Med* 51:407–421
- Faix DJ, Sherman SS, Waterman SH (2009) Rapid-test sensitivity for novel swine-origin influenza A (H1N1) virus in humans. *New Engl J Med* 361:728–729
- Gavin P, Thomson RB Jr (2003) Review of rapid diagnostic tests for influenza. *Clin Appl Immunol Rev* 4(3):151–172
- Gijs MAM (2004) Magnetic bead handling on-chip: new opportunities for analytical applications. *Microfluid Nanofluid* 1:22–40
- Grodzinski P, Liu R, Yang J, Ward MD (2004) Microfluidic system integration in sample preparation chip-sets-a summary. In: *Proceedings of the 26th annual international conference of the IEEE EMBS*, pp 2615–2618
- Hawkins TL, O'Connor-Morin T, Roy A, Santillan C (1994) DNA purification and isolation using a solid-phase. *Nucleic Acids Res* 22(21):4543–4544
- Hindiyeh M, Levy V, Azar R, Varsano N, Regev L, Shalev Y, Grossman Z, Mendelson E (2005) Evaluation of a multiplex real-time reverse transcriptase PCR assay for detection and differentiation of influenza viruses A and B during the 2001–2002 influenza season in Israel. *J Clin Microbiol* 43(2):589–595

- Huang Y, Mather EL, Bell JL, Madou M (2002) MEMS-based sample preparation for molecular diagnostics. *Anal Bioanal Chem* 372: 49–65
- Hurt AC, Baas C, Deng YM, Roberts S, Kelso A, Barr IG (2009) Performance of influenza rapid point-of-care tests in the detection of swine lineage A (H1N1) influenza viruses. *Influenza Other Respi Viruses* 3(4):171–176
- Johnson NP, Mueller J (2002) Updating the accounts: global mortality of the 1918–1920. Spanish influenza pandemic. *Bull Hist Med* 76(1):105–115
- Jungell-Nortamo A, Syvänen AC, Luoma P, Söderlund H (1988) Nucleic acid sandwich hybridization: enhanced reaction rate with magnetic microparticles as carriers. *Mol Cell Probes* 2(4): 281–288
- Kamol S, Sunchai P, Thaweesak C, Rujipat S, Alongkorn A, Thaweesak S, Arunee C, Pornchai C, Salin C, Apiradee T, Yong P (2008) Typing (A/B) and subtyping (H1/H3/H5) of influenza A viruses by multiplex real-time RT-PCR assays. *J Virol Methods* 152:25–31
- Li JH, Tang CH, Song CY, Chen MJ, Feng ZY, Pan YJ (2006) A simple, rapid and effective method for total RNA extraction from *Lentinula edodes*. *Biotechnol Lett* 28(15):1193–1197
- Li SK, Lin CH, Chen YT, Lee LH, Liu HJ (2008) Development of a reliable assay protocol for identification of diseases (RAPID)-bioactive amplification with probing for detection of avian reovirus. *J Virol Methods* 149(1):35–41
- Lien KY, Liu CJ, Lin YC, Kuo PL, Lee GB (2009) Extraction of genomic DNA and detection of single nucleotide polymorphism genotyping utilizing an integrated magnetic bead-based microfluidic platform. *Microfluid Nanofluid* 6:539–555
- Liu CJ, Lien KY, Weng CY, Shin JW, Chang TY, Lee GB (2009) Magnetic-bead-based microfluidic system for ribonucleic acid extraction and reverse transcription processes. *Biomed Microdevices* 11:339–350
- Matsuzaki Y, Katsushima N, Nagai Y, Shoji M, Itagaki T, Sakamoto M, Kitaoka S, Mizuta K, Nishimura H (2006) Clinical features of influenza C virus infection in children. *J Infect Dis* 193(9): 1229–1235
- McCalla SE, Ong C, Sarma A, Opal SM, Artenstein AW, Tripathi A (2012) A simple method for amplifying RNA targets (SMART). *J Mol Diagn* 14(4):328–335
- Medina RA, Garcia-Sastre A (2011) Influenza A viruses: new research developments. *Rev Microbiol* 9:590–603
- Payungporn S, Chutinimitkul S, Chaisingh A, Damrongwanapokin S, Buranathai C, Amonsin A, Theamboonlers A, Poovorawan Y (2006) Single step multiplex real-time RT-PCR for H5N1 influenza A virus detection. *J Virol Methods* 113:143–147
- Siavashi MR, Taherkhani H, Rezaei K, Deligani MRR, Assmar M (2005) Comparison of Dot-ELISA and sandwich ELISA diagnostic tests in detection of human hydatidosis. *Iran Biomed J* 9(2):91–94
- Simonsen L, Clarke MJ, Williamson GD, Stroup DF, Arden NH, Schonberger LB (1997) The impact of influenza epidemics on mortality: introducing a severity index. *Am J Public Health* 87(12):1944–1950
- Smith AB, Mock B, Meleau R, Colarusso P, Willis DE (2003) Rapid detection of influenza A and B viruses in clinical specimens by Light Cycler real time RT-PCR. *J Clin Virol* 28(1):51–58
- Smith GJ, Vijaykrishna D, Bahl J, Lycett SJ, Worobey M, Pybus OG, Ma SK, Cheung CL, Raghvani J, Bhatt S, Peiris JS, Guan Y, Rambaut A (2009) Origins and evolutionary genomics of the 2009 swine-origin H1N1 influenza A epidemic. *Nature* 459(7250):1122–1125
- Thontiravong A, Payungporn S, Keawcharoen J, Chutinimitkul S, Wattanodorn S, Damrongwanapokin S, Chaisingh A, Theamboonlers A, Poovorawan Y, Oraveerakul K (2007) The single-step multiplex reverse transcription-polymerase chain reaction assay for detecting H5 and H7 avian influenza A viruses. *Tohoku J Exp Med* 211(1):75–79
- Vasoo S, Stevens J, Singh K (2009) Rapid antigen tests for diagnosis of pandemic (swine) influenza A/H1N1. *Clin Infect Dis* 49:1090–1093
- Vilkner T, Janasek D, Manz A (2004) Micro total analysis systems. Recent developments. *Anal Chem* 76:3373–3385
- Wang CH, Lien KY, Hung LY, Lei HY, Lee GB (2012) Integrated microfluidic system for multiple subtyping of influenza virus by using molecular diagnosis approach. *Microfluid Nanofluid* 13(1):113–123
- Webster RG, Bean WJ, Gorman OT (1992) Evolution and ecology of influenza-A virus. *Rev Microbiol* 56(1):152–179
- Weng CH, Lien KY, Yang SY, Lee GB (2011a) A suction-type, pneumatic microfluidic device for liquid transport and mixing. *Microfluid Nanofluid* 10:301–310
- Weng CH, Lien KY, Yang SY, Lee GB (2011b) A suction-type, pneumatic microfluidic device for liquid transport and mixing. *Microfluid Nanofluid* 10:301–310
- Witthaya P, Piyathida P, Jarika M, Yong P, Sunchai P (2011) Molecular detection and subtyping of human influenza A virus based on multiplex RT-PCR assay. *Int Res J Biotech* 2(5): 085–092
- Yang YN, Hsiung SK, Lee GB (2009) A pneumatic micropump incorporated with a normally closed valve capable of generating a high pumping rate and a high back pressure. *Microfluid Nanofluid* 6:823–833
- Zhang C, Xing D (2010) Single-molecule DNA amplification and analysis using microfluidics. *Chem Rev* 110:4910–4947
- Zheng HJ, Tao ZH, Cheng WF, Piessens WF (1990) Comparison of dot-ELISA with sandwich ELISA for the detection of circulating antigens in patients with bancroftian filariasis. *Am J Trop Med Hygiene* 42:546–549
- Zhu X, Yu W, McBride R, Li Y, Chen LM, Donis RO, Tong S, Paulson JC, Wilson LA (2012) Hemagglutinin homologue from H17N10 bat influenza virus exhibits divergent receptor-binding and pH-dependent fusion activities. *Proc Natl Acad Sci* 110(4): 1458–1463